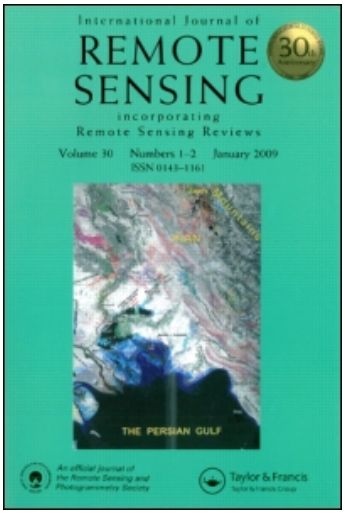

International Journal of Remote Sensing
Publication details, including instructions for authors and subscription information:
http://www.informaworld.com/smpp/title~content=t713722504

An alternative method for in-flight absolute radiometric calibration of thermal infrared channels of Chinese geostationary meteorological satellites

Jinjun Tong [a]; S. J. Déry [a]; Yun Chen [b]; Bo Hu [c]
[a] Environmental Science and Engineering Program, University of Northern British Columbia, Prince George, BC, Canada [b] National Meteorological Centre, China Meteorological Administration, Beijing, China [c] Department of Human Resources, China Meteorological Administration, Beijing, China

Online publication date: 23 February 2010

To cite this Article Tong, Jinjun, Déry, S. J., Chen, Yun and Hu, Bo(2010) 'An alternative method for in-flight absolute radiometric calibration of thermal infrared channels of Chinese geostationary meteorological satellites', International Journal of Remote Sensing, 31: 3, 791 — 803
To link to this Article: DOI: 10.1080/01431160902897841
URL: http://dx.doi.org/10.1080/01431160902897841

International Journal of Remote Sensing
Vol. 31, No. 3, 10 February 2010, 791–803

Taylor & Francis
Taylor & Francis Group

An alternative method for in-flight absolute radiometric calibration of thermal infrared channels of Chinese geostationary meteorological satellites

JINJUN TONG*†, S. J. DÉRY†, YUN CHEN*‡ and BO HU§

†Environmental Science and Engineering Program, University of Northern British Columbia, Prince George, BC, V2N 4Z9 Canada

‡National Meteorological Centre, China Meteorological Administration, Beijing 100081, China

§Department of Human Resources, China Meteorological Administration, Beijing 100081, China

(*Received 8 July 2008; in final form 16 March 2009*)

The aim of this study was to explore the feasibility of an alternative method for in-flight absolute radiometric calibration of the thermal infrared (TIR) channels of the Chinese meteorological satellites FengYun-2B (FY-2B) and FengYun-2C (FY-2C). The alternative method substituted radiosonde atmospheric profiles with those from the National Centers for Environmental Prediction (NCEP) reanalysis and the water surface brightness temperatures from TIR radiometers (CE312) with those from an automated hydrometeorological buoy (AHMB) system over Qinghai Lake (QHL), China. These data were then used to calculate the calibration coefficients and their uncertainty for the TIR channels of FY-2B and FY-2C. The at-sensor radiance (ASR) and at-sensor brightness temperature (ASBT) of the TIR channels of FY-2B and FY-2C were calculated by using 14 atmospheric profiles as measured by radiosonde over QHL in August 2003 and the corresponding NCEP reanalysis data, respectively. In addition, we conducted sensitivity tests to different atmospheric profiles of varying relative humidity and air temperatures on the ASR and ASBT of the TIR channels of FY-2B and FY-2C. Differences in gains between the regular and alternative methods are less than 0.005 mW m^{-2} sr^{-1} cm^{-1} DN^{-1}. The sensitivity tests show that the ASR and ASBT are more sensitive to the relative humidity than the temperature in the atmospheric profile. Our results show that the proposed alternative method, of which the uncertainty is about 1.5 K for the TIR channels of FY-2B and FY-2C, is feasible for the TIR channels of various remote sensors. One of the major benefits of this alternative method is the potential for more frequent, reliable and inexpensive calibrations of the TIR sensors in operational conditions.

1. Introduction

The thermal infrared (TIR) channels of remote sensing platforms are used to study phenomena such as urban heat island effects, to classify cloud types, and to track sea, land and snow surface temperatures through quantitative applications that are based on the high precision of absolute radiometric calibration (Key *et al.* 1997, Sobrino

*Corresponding author. Email: jtong@unbc.ca; shenyun73@hotmail.com

International Journal of Remote Sensing
ISSN 0143-1161 print/ISSN 1366-5901 online
http://www.tandf.co.uk/journals
DOI: 10.1080/01431160902897841

et al. 2003, 2004). The methods of calibration for the TIR channels of satellite sensors include pre-launch, on-board and in-flight calibrations, which have their different limitations for calibration (Barnes *et al.* 1998, 2000, Minnis *et al.* 2002). A pre-launch calibration normally detects the spectral response range, the calibration coefficients and the performance of components before the satellite is sent into orbit. An on-board calibration system that detects changes in the calibration coefficients as well as the performance of the components is also mounted on the remote sensor systems. Some of the latest remote sensors, such as the Moderate Resolution Imaging Spectroradiometer (MODIS), also have an on-board calibration system to detect the spectral response (Xiong and Barnes 2006). However, because the absolute radiometric calibration coefficients for TIR channels are highly sensitive to the operational environment, which may be very different from the experimental one of the pre-launch calibration, they cannot be adopted for operational periods (Tong 2004).

The Chinese geostationary meteorological satellite FengYun-2B (FY-2B) was launched in June 2000; it has a multichannel scanning radiometer (MSR) with a TIR channel covering 10.5–12.0 μm. The FengYun-2C (FY-2C) has been operational since October 2004; it has an MSR and two split-window TIR channels covering 10.3–11.3 μm (TIR1) and 11.5–12.5 μm (TIR2). For both of these satellites, the on-board calibration is implemented by inserting a calibration mirror into the optical path to measure the on-board blackbody. Therefore, the calibration optical path does not include the entire optical path that is used to view Earth targets. The on-board calibration system only calibrates the rear part of the entire optical path of the MSR, and is therefore only a relative calibration. In a previous study we found that the difference in at-sensor brightness temperature (ASBT) calculated by the on-board calibration coefficients and in-flight absolute radiometric calibration coefficients ranged from 1 to 15 K for the TIR channels of FY-2C (Tong *et al.* 2009). Therefore, in-flight absolute radiometric calibration is necessary to validate the pre-launch and on-board calibrations. In the current study various independent calibration methods are explored to avoid the system errors in the pre-launch, on-board, and in-flight calibration methods.

For in-flight calibration of the TIR channels, an experimental site consisting of a large, homogeneous body of water such as Qinghai Lake (QHL) in China is desirable. QHL is located to the northeast of the Qinghai-Tibet Plateau in China, with the centre at approximately 36° 45′ N, 100° 22′ E. It covers an area of about 4635 km^2 at an elevation of 3196 m. QHL is considered an ideal calibration site for the TIR channels for the following reasons: (1) its water is of high quality, with a reflectivity of 4% and 1% for the visible and TIR channels, respectively; (2) its surface temperature distribution is homogeneous, with a range of less than 1 K over its entire surface; and (3) it is located at a relatively high elevation with clean air, thus requiring less atmospheric correction for calibration. The water surface BT and atmospheric profiles are necessary to run the atmospheric transfer model MODTRAN 5.0 to calculate the calibration coefficients when the TIR channels obtain clear-sky images of the test sites. The in-flight calibration method has been used previously to successfully calibrate TIR channels (Palmer 1993, Slater *et al.* 1996, Wang *et al.* 2001, Tong *et al.* 2004a,b, 2005, 2009, Rong *et al.* 2007). This method, however, can only be carried out about twice a year because of the associated high labour requirements and monetary costs. This paper proposes an alternative method to perform an in-flight calibration of the TIR channels. We used the surface water temperatures of QHL, measured by the automated hydrometeorological buoy (AHMB) system, and the atmospheric profiles over

QHL obtained from the National Centers for Environmental Prediction (NCEP) reanalysis to substitute *in-situ* field data to obtain more frequent and reliable absolute radiometric calibration coefficients. This alternative method was adopted to calculate the calibration coefficients of the TIR channels of FY-2B and FY-2C. The *in-situ* data were compared with the alternative method to test its feasibility for in-flight absolute radiometric calibration of TIR channels. Although FY-2B ceased to operate after the launch of FY-2C, this alternative method was used on both platforms to compare the effects of the atmospheric profiles on the calibration between the TIR channel of FY-2B and the split-window TIR channels of FY-2C.

2. Data

2.1 *Experimental data*

To verify the performance of the TIR channels of FY-2B and FY-2C, two research groups of about 20 scientists led by the National Satellite Meteorological Centre, China conducted calibration experiments over QHL from 5 to 25 August 2003 and from 10 to 30 June 2005. Because of the frequent cloudiness of the region, we obtained only one successful experimental day each year. This occurred at 10:00 a.m. (local time) on 15 August 2003 and at 11:00 a.m. (local time) on 25 June 2005 for FY-2B and FY-2C, respectively. The water surface BTs of QHL measured by the TIR radiometers (CE312) were 288.1, 286.1 and 286.3 K for TIR of FY-2B, TIR1 of FY-2C and TIR2 of FY-2C, respectively. The atmospheric profiles over QHL were detected concurrently with sounding balloons. The images and digital numbers (DNs) of QHL of the TIR channels of FY-2B and FY-2C during the two *in-situ* experiments were also extracted.

2.2 *Data from AHMB and NCEP*

The QHL AHMB system is one component of the Weather and Environment Observation Systems in the China Radiometric Calibration Site for Remote Sensing Satellites. The AHMB continually measures five meteorological parameters (air temperature, atmospheric pressure, humidity, wind speed and wind direction) and two hydrological characteristics (water surface temperature and salinity) at a fixed position once every hour from April to October when the QHL is free from lake ice (Jin and Tan 2001). In the current study, the water surface temperatures were used to substitute the water surface BTs of QHL. The NCEP reanalysis data are gridded globally at $1^\circ \times 1^\circ$ with 26 vertical layers of various meteorological parameters that are available at 00, 06, 12 and 18 UTC (Kalnay *et al.* 1996). In this paper, the NCEP reanalysis data near 37° N, 100° E were considered representative of the humidity and temperature profiles above QHL.

3. Theory of calibration

There are three different energy inputs included in the at-sensor radiance (ASR) received by TIR detectors when they view the lake. The first part of the ASR comes from the thermal radiation of the water surface, which is attenuated by the atmosphere. The energy of this part depends on the temperature of the water surface, the emissivity of the water, and the transmissivity of the atmospheric path between the satellite and the body of water. The second part of the ASR is the path radiance of the atmosphere, which is related to the content of the absorptive components and the

physical characteristics of the atmosphere. The third part of the ASR is the energy reflected from the water surface. The top of atmosphere (TOA) radiance at a given wavelength λ is represented by:

$$L_T(\lambda) = L_1(\lambda) + L_2(\lambda) + L_3(\lambda) \tag{1}$$

where the TOA thermal radiance of the water surface is expressed by:

$$L_1(\lambda) = \tau_a(\lambda) L_{lake}(\lambda) \tag{2}$$

Here $\tau_a(\lambda)$ is the atmospheric transmittance at wavelength λ from the target to the TOA, and $L_{lake}(\lambda)$ is the radiance from the water surface along the view angle. The path radiance of the atmosphere, $L_{up}(\lambda)$, along the view angle provides the second component of the TOA radiance such that:

$$L_2(\lambda) = L_{up}(\lambda) \tag{3}$$

Next, the TOA radiance reflected by the water surface at wavelength λ is obtained from:

$$L_3(\lambda) = \rho_{lake}(\lambda)\tau_a(\lambda) L_{down}(\lambda) \tag{4}$$

where ρ_{lake} is the reflectance of the water surface and $L_{down}(\lambda)$ is the atmospheric radiance reflected along the view angle. As the QHL water surface is treated as an absolute blackbody throughout the TIR wavelength, $L_3(\lambda)$ is negligible compared to the other two terms (Wang *et al.* 2001). According to the analyses above, the TOA radiance at a given wavelength λ may then be expressed as:

$$L_T(\lambda) = \tau_a(\lambda) L_{lake}(\lambda) + L_{up}(\lambda) \tag{5}$$

Then the ASR of the TIR channels, L_{ASR}, is calculated by integrating $L_T(\lambda)$ over the spectral response of channels $S(\lambda)$ throughout the wavelength range such that:

$$L_{ASR} = \frac{\int L_T(\lambda) S(\lambda) \mathrm{d}\lambda}{\int S(\lambda) \mathrm{d}\lambda} \tag{6}$$

Although there is a non-linear component of a few per cent in the very low ranges of the TIR channels, the pre-launch calibration experiments of the FY-2 channels did not provide the non-linear calibration coefficients. These are difficult to assess from in-flight conditions so a linear calibration was adopted for FY-2. Because of the linear relationship between ASR and the response of the detectors, the calibration coefficients for a given TIR channel i can be given as:

$$L_{ASRi} = G_i\, DN_i + I_i \tag{7}$$

where L_{ASRi} represents the ASR of channel i in units of mW m^{-2} sr^{-1} cm^{-1}, DN$_i$ represents the digital number, and G_i and I_i represent the gain and offset with units of mW m^{-2} sr^{-1} cm^{-1} DN^{-1} and mW m^{-2} sr^{-1} cm^{-1}, respectively.

To calculate the calibration coefficients, two groups of ASR and DN during satellite scans of the QHL are required. A field experiment was carried out over QHL at the same time as satellite overpasses to measure the upward radiance BT with TIR radiometers (CE312) and the atmospheric profiles with sounding balloons. The measured data were input into the atmospheric transfer model MODTRAN 5.0 to calculate the ASR and ASBTs. These are considered as high values of the linear calibration curve, whereas the ASR of deep space is considered zero such that it represents a low value of the linear calibration curve. Combining the two groups of

ASR and ASBT with the corresponding DN, the calibration coefficients were obtained. Before the field experiment, the CE312 was calibrated using a portable blackbody calibration source (M340) produced by Mikron Infrared Inc. (Rong *et al.* 2007). The accuracy of the M340 is 0.2 K with National Institute of Standards and Technology (NIST) traceable certification (http://www.mikroninfrared.com/literature/blackbody.pdf). Therefore, the in-flight calibration based on the measurement of CE312 is an absolute radiometric calibration.

4. Calculation of absolute calibration coefficients

To obtain the ASR of the TIR channels according to equations (5) and (6), $L_{\text{lake}}(\lambda)$, $\tau_a(\lambda)$ and $L_{\text{up}}(\lambda)$ must first be calculated. The water surface BT of QHL measured by CE312 and atmospheric profiles were input into MODTRAN5.0 to calculate the TOA radiance. Two different atmospheric profiles including radiosonde measurements and the corresponding NCEP reanalysis data were adopted to compare the calibration coefficients obtained when using different atmospheric profiles. Figure 1 shows the TOA radiance over the whole spectral range of the TIR channels of FY-2B and FY-2C calculated by different atmospheric profiles on two separate days. At 10:00 a.m. (local time) on 15 August 2003, the different atmospheric profiles introduced significant differences (of up to 40 mW m^{-2} sr^{-1} cm^{-1}) in the TOA radiance in the water vapour absorption range between 650 and 700 cm^{-1} and 1000 and 1070 cm^{-1}; however, in the TIR channels, the TOA radiances were almost the same despite

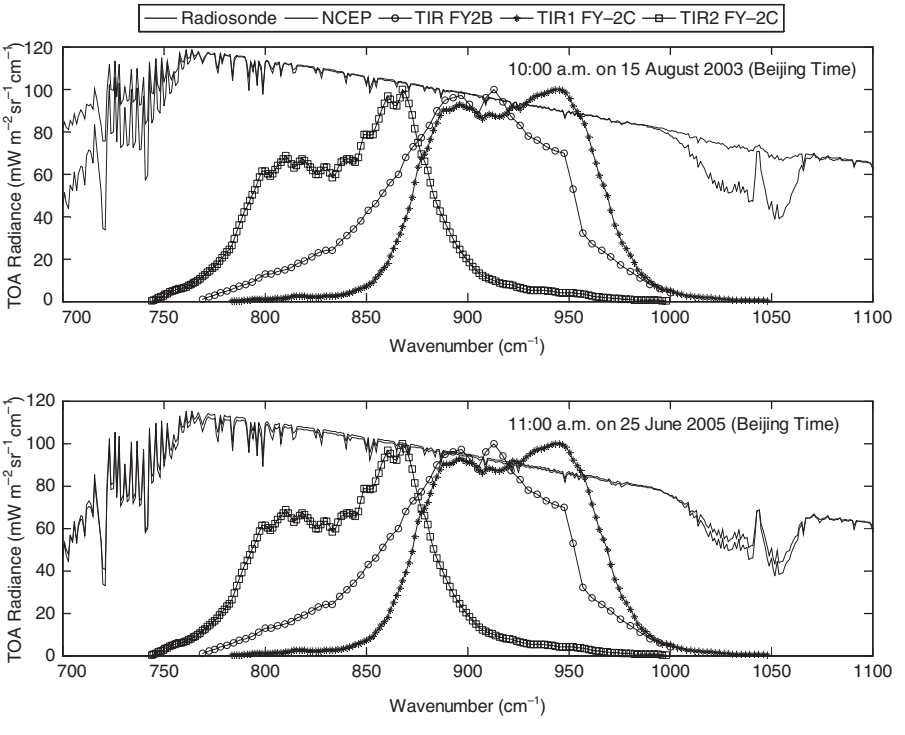

Figure 1. Top of atmosphere (TOA) radiance for the two field experiments over QHL calculated from the atmospheric profiles and the corresponding NCEP reanalysis data and the spectrum response of the TIR channels of FY-2B and FY-2C.

Table 1. The at-sensor radiance (ASR) and brightness temperature (ASBT) of the TIR channels of FY-2B and FY-2C calculated by the atmospheric profiles measured in the two field experiments over QHL and corresponding NCEP reanalysis data.

	ASR (mW m^{-2} sr^{-1} cm^{-1})			ASBT (K)		
Atmospheric profiles	TIR FY-2B	TIR1 FY-2C	TIR2 FY-2C	TIR FY-2B	TIR1 FY-2C	TIR2 FY-2C
Radiosonde	97.88	90.45	101.72	287.42	285.02	284.05
NCEP	98.38	91.35	103.34	287.74	285.63	285.08

the different atmospheric profiles. At 11:00 a.m. (local time) on 25 June 2005, the TOA radiances for different atmospheric profiles were similar even in the water vapour absorption ranges. The spectral responses show that the TIR2 of FY-2C covers the water vapour absorption band of 1000–1070 cm^{-1}, which affects the calibration uncertainty because of the different atmospheric profiles; however, TIR1 of FY-2B and TIR1 of FY-2C lie outside the water vapour absorption wavelength ranges. The ASR, ASBT and calibration coefficients for the TIR channels are shown in tables 1 and 2. The differences in ASR introduced by the different atmospheric profiles are 0.5, 0.9 and 1.6 mW m^{-2} sr^{-1} cm^{-1} for TIR of FY-2B, TIR1 of FY-2C and TIR2 of FY-2C, respectively. The difference in gains are 0.0001, 0.002 and 0.004 mW m^{-2} sr^{-1} cm^{-1} DN^{-1} for TIR of FY-2B, TIR1 of FY-2C and TIR2 of FY-2C, respectively.

5. Uncertainty of calibration

The proposed alternative method substitutes the water surface BTs measured by CE312 and atmospheric profiles measured by radiosonde with water surface temperatures assessed by AHMB and atmospheric profiles from NCEP reanalysis data. The uncertainty in the original method consists of the surface radiance of QHL, the calculation of the atmospheric radiative transfer and the radiance of the TIR channels and the extraction of the DNs. The original method has 1 K uncertainty, which remains acceptable based on the results of the TIR channels of HaiYang-1 (HY-1) for oceanic applications, and FY-1C and FY-2B for meteorological applications (Wang *et al.* 2001, Tong *et al.* 2004b). For the calibration coefficients based on the alternative methods, the uncertainty arises mainly from the measurement of the water surface temperature and atmospheric profile and calculation of the atmospheric

Table 2. The gain and offset of the TIR channels of FY-2B and FY-2C calculated by the atmospheric profiles measured in the two field experiments over QHL and corresponding NCEP reanalysis data.

	Gain (mW m^{-2} sr^{-1} cm^{-1} DN^{-1})			Offset (mW m^{-2} sr^{-1} cm^{-1})		
Atmospheric profiles	TIR FY-2B	TIR1 FY-2C	TIR2 FY-2C	TIR FY-2B	TIR1 FY-2C	TIR2 FY-2C
Radiosonde	–0.7715	–0.2128	–0.2691	177.4539	211.9633	266.7762
NCEP	–0.7716	–0.2149	–0.2734	177.4743	214.0698	271.2041

radiative transfer. Therefore, only the uncertainty arising from the different temperature and relative humidity profiles is discussed here. Improvements in the atmospheric radiative transfer model and the uncertainty associated with other atmospheric parameters in the model are beyond the scope of this paper. These uncertainties and sensitivity tests of the ASR and ASBT based on different atmospheric profiles are discussed in the following sections.

5.1 *Comparison between BT and temperatures over QHL*

In the alternative method, the water surface temperature of QHL from AHMB is taken as the BT based on the assumption that the water surface of QHL is a perfect blackbody with an emissivity of 1. However, the difference between the water surface BT measured by CE312 and the water surface temperature from AHMB leads to uncertainty in the calculation of ASR. During August 2003, CE312 was used to measure the water surface BT at QHL and compared to the corresponding surface temperatures measured by AHMB (figure 2). The temperatures range from 287.2 K to 289.2 K. The data show that only two out of 10 absolute differences between surface BTs and surface temperatures reach about 0.6 K, whereas the remaining eight out of ten absolute differences are less than 0.5 K with a root mean square (RMS) of 0.4 K. As the upward radiance BT measured by CE312 includes the influence of the reflectance of the water surface in the TIR channels, the uncertainty associated with the water surface temperature measured by AHMB already includes the reflective effects of the water surface.

5.2 *Comparison between different atmospheric profiles*

In the alternative method proposed here, the radiosonde profiles were replaced by profiles from NCEP reanalysis data. These were then input into MODTRAN5.0 to calculate the atmospheric transmission and path radiance. The uncertainty of the atmospheric profiles from the NCEP reanalysis data leads to the uncertainty of the calibration coefficients. There were only 14 radiosonde profiles taken over QHL from August 2003 that were substituted by those inferred from the NCEP reanalysis data. The two types of atmospheric profiles were used to run MODTRAN5.0 to calculate the ASR and ASBT for TIR channels of FY-2B and FY-2C, respectively. The water

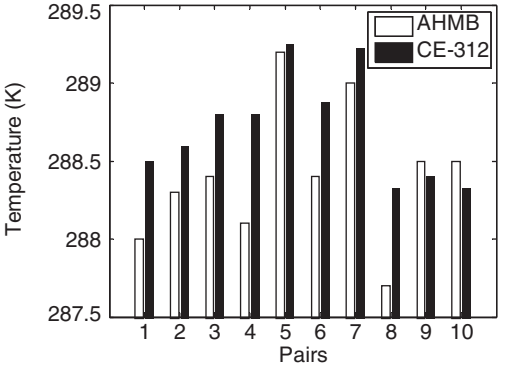

Figure 2. Water surface temperatures measured by AHMB and brightness temperatures measured by CE312 in August 2003.

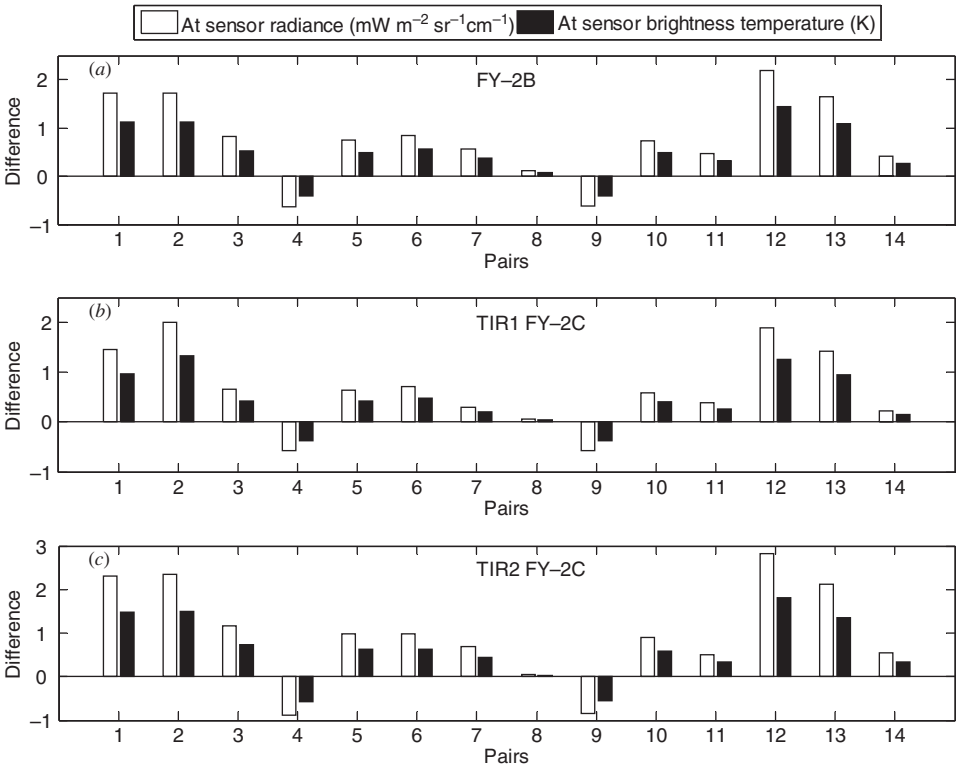

Figure 3. Differences between at-sensor radiance and brightness temperature of TIR of (*a*) FY-2B, (*b*) TIR1 of FY-2C and (*c*) TIR2 of FY-2C calculated from sounding data and NCEP reanalysis data.

surface BT was set as 288.1 K. In the 14 comparisons, the atmospheric profiles of NCEP reanalysis data replaced the radiosonde ones, leading to differences in ASR and ASBT (figure 3). The absolute values of the differences in ASR are small, ranging from 0.05 to 2.82 mW m^{-2} sr^{-1} cm^{-1}. The RMS values for ASR are 1.16, 0.98 and 1.368 mW m^{-2} sr^{-1} cm^{-1} for TIR of FY-2B, TIR1 of FY-2C and TIR2 of FY-2C, respectively. The absolute values of differences in ASBT are also small, ranging from 0.03 to 1.81 K. The RMS for ASBT are 0.76, 0.64 and 0.98 K for TIR of FY-2B, TIR1 of FY-2C and TIR2 of FY-2C, respectively.

5.3 *Sensitivity tests of ASR and ASBT*

Although we compared the results based on 14 different atmospheric profiles, they remain insufficient to assess their impact on the ASR and ASBT. Therefore, three additional tests were performed with the MODTRAN 5.0 model to explore how the atmospheric profiles affect the calibration of the TIR channels. In these tests, the original values of the relative humidity and temperature at each level were altered to obtain substantially different atmospheric profiles. The vertical profile measured at 10:00 a.m. on 15 August 2003 (local time) was adopted as the original atmospheric profile (figure 4).

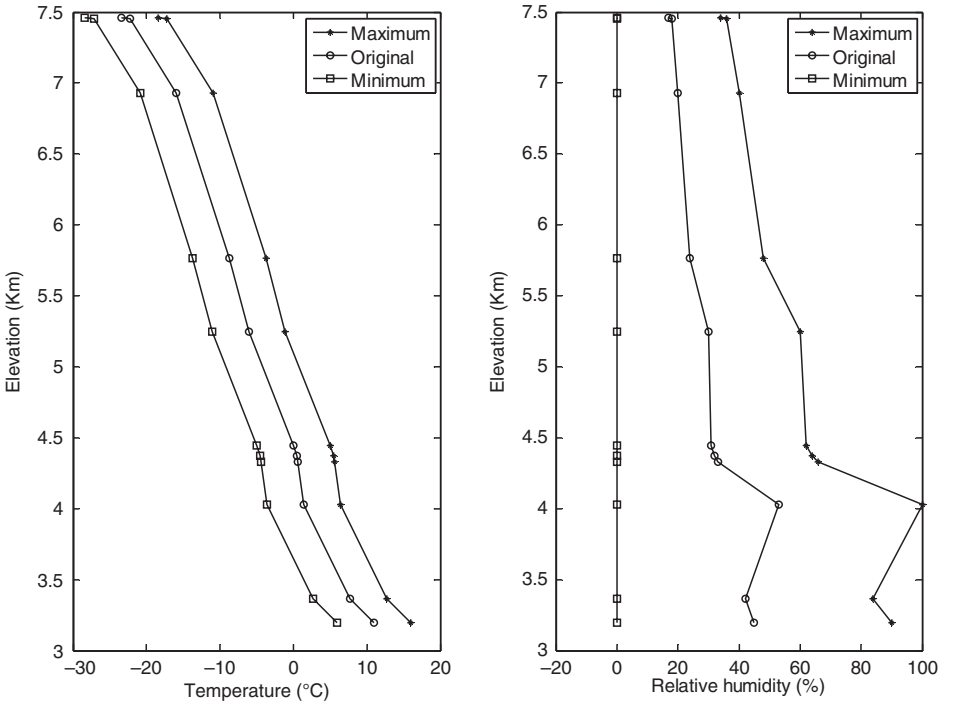

Figure 4. Vertical profiles of air temperature and relative humidity measured by radiosonde over QHL at 10:00 a.m. (local time) on 15 August 2003 and the maximum and minimum vertical profiles of the air temperature and relative humidity in the sensitivity test.

5.3.1 Sensitivity tests to relative humidity In this test, the temperatures at different levels in the atmospheric column remained constant. However, the profiles of relative humidity varied between 0% and 200% from their original values using intervals of 20%. Then 11 different atmospheric profiles with different relative humidity and identical temperatures were constructed. Where the original atmospheric profiles were multiplied by 0%, all relative humidities were taken as zero. In situations where the original atmospheric profiles were multiplied by 200%, the relative humidities ranged from over 30% to a maximum of 100% (figure 4). The ASR and ASBT decreased with increasing relative humidity because of the greater absorption by water vapour (figure 5). However, for TIR of FY-2B, TIR1 of FY-2C and TIR2 of FY-2C, the differences in ASR between the atmospheric profiles with 0% relative humidity and double relative humidity were 2.9, 2.3 and 4.3 mW m^{-2} sr^{-1} cm^{-1} with the differences of ASBT about 1.9, 1.5 and 2.7 K, respectively.

5.3.2 Sensitivity tests to air temperature In these tests, values of relative humidity remained fixed whereas temperatures in the atmospheric column were modified by adding departures ranging from –5°C to 5°C in 1°C increments (figure 4). Then 11 different atmospheric profiles with varying air temperatures and identical relative humidity were constructed. Although the ASR and ASBT decreased with increasing air temperatures, their differences over the range of air temperatures were at most 0.1 mW m^{-2} sr^{-1} cm^{-1} and 0.1 K for all TIR channels (figure 6).

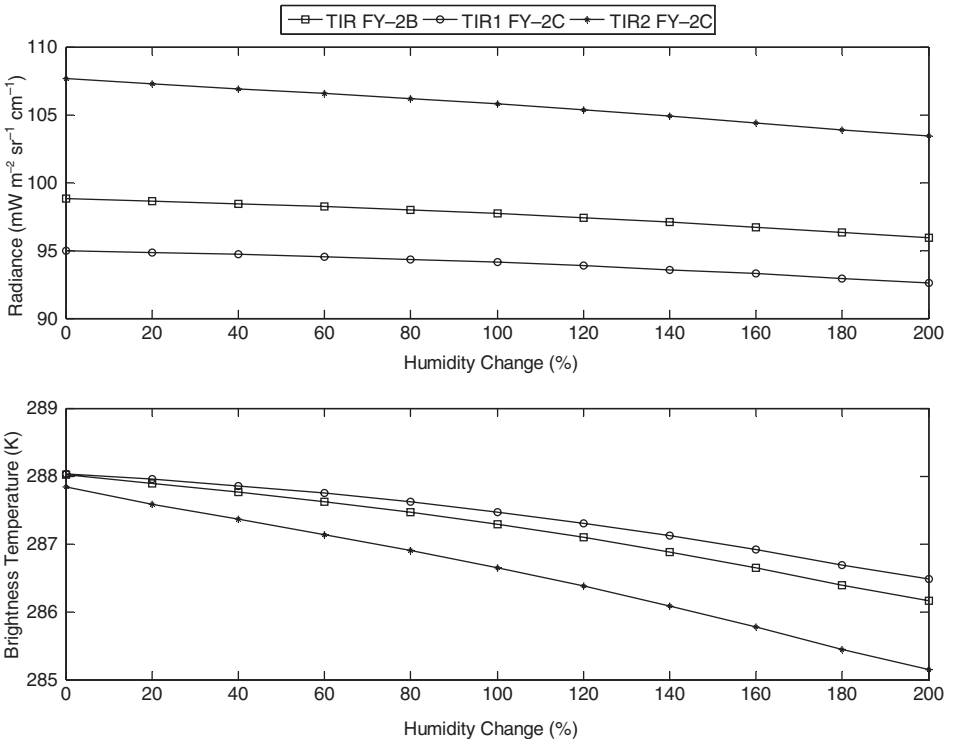

Figure 5. At-sensor radiance and brightness temperatures of the TIR channels of FY-2B and FY-2C with the change in relative humidity in the atmospheric profiles.

5.3.3 Sensitivity tests to both relative humidity and air temperature In the final sensitivity test, the relative humidity and air temperature at different levels of the atmospheric column were changed simultaneously. Thus, the relative humidities were altered by multiplying coefficients ranging from 0% to 200% at intervals of 20% and the air temperatures were concurrently modified by adding departures from –5°C to 5°C at 1°C intervals. The resulting 11 atmospheric profiles of varying relative humidity and air temperature yield a range of ASR and ASBT values (figure 7). The ASR and ASBT decreased with increasing humidity and air temperatures because of the absorption of water vapour. However, for TIR of FY-2B, TIR1 of FY-2C and TIR2 of FY-2C, the differences in ASR between the atmospheric profiles with 0% relative humidity and 200% times relative humidity were 2.8, 2.3 and 4.0 mW m^{-2} sr^{-1} cm^{-1} with the difference in ASBT about 1.8, 1.2 and 2.6 K, respectively.

5.4 *Estimation of uncertainty*

Combining the RMS of different factors such as measurements of temperature over QHL, calculation of atmospheric radiative transfer and uncertainty of regular in-flight absolute radiometric calibration methods, the total uncertainty of the alternative absolute radiometric calibration of TIR channels can be estimated according to equation (8) (Slater *et al*. 1996):

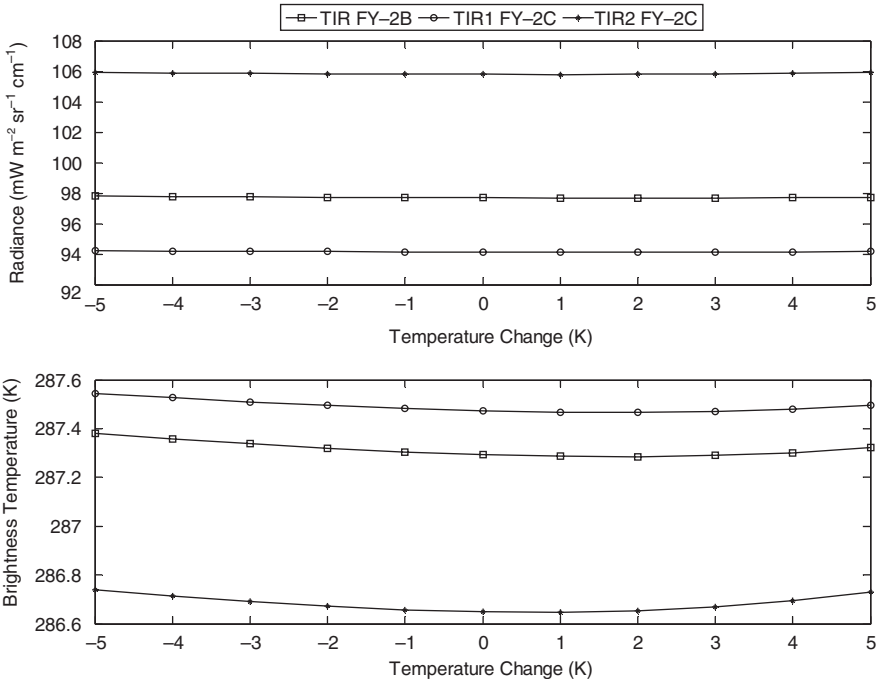

Figure 6. At-sensor radiance and brightness temperatures of the TIR channels of FY-2B and FY-2C with the change in temperature in the atmospheric profiles.

$$\text{Uncertainty} = \sqrt{\sum_{i=1}^{n} \text{RMS}_i} \tag{8}$$

However, the total estimated uncertainty excludes a non-linear component arising at lower ranges of the FY-2 TIR channels because of a lack of pre-launch non-linear calibration experiments. The estimated total uncertainties are 1.47, 1.43 and 1.54 K for TIR of FY-2B, TIR1 of FY-2C and TIR2 of FY-2C, respectively.

6. Conclusions

This study demonstrates that the calibration coefficients for the TIR channels of FY-2B calculated using atmospheric profiles from either radiosonde soundings or NCEP reanalysis data yield consistent results. Comparison of ASR and ASBT at different atmospheric profiles indicate that those based on the NCEP reanalysis data over QHL can be adopted to calibrate accurately the TIR channels of FY-2B and FY-2C. Furthermore, comparisons between the water surface BT from CE312 and the water surface temperature from AHMB indicate that the latter has sufficient precision to be used in the calibration of the TIR channels. The sensitivity tests show that the TIR channels of FY-2B and FY-2C are not highly responsive to the atmospheric profiles because these channels avoid the water vapour absorption windows. Comparisons between the TIR channel of FY-2B and the split-window channels of TIR1 and TIR2 of FY-2C show that TIR1 of FY-2C has the lowest sensitivity to the atmospheric profiles followed by TIR of FY-2B and TIR2 of FY-2C. The uncertainties of the alternative method are 1.47, 1.43 and 1.54 K for TIR of FY-2B, TIR1 of

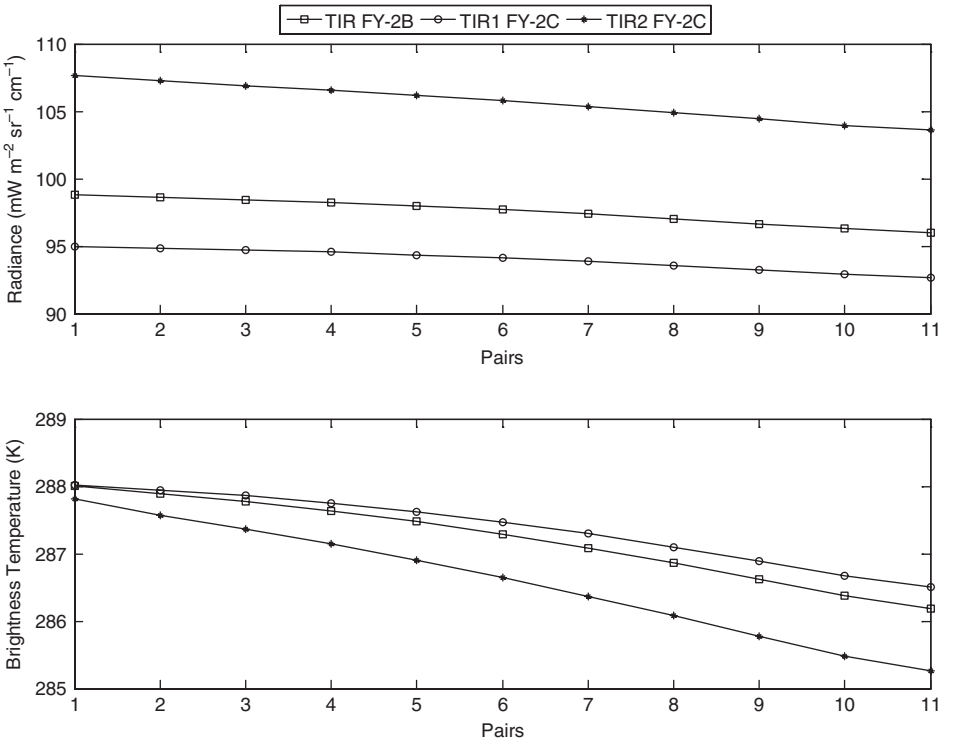

Figure 7. At-sensor radiance and brightness temperatures of the TIR channels of FY-2B and FY-2C with the change in relative humidity and temperature in the atmospheric profiles.

FY-2C and TIR2 of FY-2C, respectively. Therefore, this alternative method for in-flight absolute radiometric calibration of the TIR channels for FY-2B and FY-2C is also feasible for additional satellite sensors as long as these do not cover the water vapour spectrum ranges. This alternative method can significantly increase the frequency and reliability of in-flight absolute radiometric calibration for TIR channels of satellite sensors at nominal costs.

Acknowledgements

We gratefully acknowledge support by the Canada Research Chair programme of the Government of Canada, the Natural Sciences and Engineering Research Council of Canada, the National Natural Science Foundation of China (No. NSFC-40675059), and the China National High Technology Research and Development Programme (863; No. 2006AA12Z103). Comments by two anonymous referees greatly improved the paper.

References

Barnes, R.A., Barnes, W.L., Lyu, C.H. and Gales, M.J., 2000, An overview of the Visible and Infrared Scanner radiometric calibration algorithm. *Journal of Atmospheric and Oceanic Technology*, **17**, pp. 395–405.

Barnes, W.L., Pangano, T.S. and Salomonson, V.V., 1998, Prelaunch characteristics of Moderate Resolution Spectroradiometer (MODIS) on EOS-AM1. *IEEE Transactions on Geoscience and Remote Sensing*, **36**, pp. 1088–1100.

Jin, Y.M. and Tan, S.X., 2001, The meteorology auto-observation system in Qinghai Lake. In *The Scientific Research Papers about China Radiometric Calibration Site for Remote Sensing Satellite*, K. Qiu (Ed.), pp. 111–120 (Beijing: Ocean Press).

Kalnay, E., Kanamitsu, M., Kistler, R., Collins, W., Deaven, D., Gandin, L., Iredell, M., Saha, S., White, G., Woollen, J., Zhu, Y., Leetmaa, A., Reynolds, B., Chelliah, M., Ebisuzaki, W., Higgins, W., Janowiak, J., Mo, K.C., Ropelewski, C., Wang, J., Jenne, R. and Joseph, D., 1996, The NCEP/NCAR 40 year reanalysis project. *Bulletin of the American Meteorological Society*, **77**, pp. 437–471.

Key, J.R., Collins, J.B., Fowler, C. and Stone, R.S., 1997, High latitude surface temperature estimates from thermal satellite data. *Remote Sensing of Environment*, **61**, pp. 302–309.

Minnis, P., Nguyen, L., Doelling, R.D., Young, F.D., Miller, F.W. and Kratz, P.D., 2002, Rapid calibration of operational and research meteorological satellite imagers. Part II: Comparison of infrared channels. *Journal of Atmospheric and Oceanic Technology*, **19**, pp. 1250–1266.

Palmer, J.M., 1993, Calibration of satellite sensors in the thermal infrared. *Proceedings of SPIE*, **1762**, pp. 108–117.

Rong, Z.G., Zhang, Y.X. and Jia, F.M., 2007, On-orbit radiometric calibration of FENGYUN geostationary meteorological satellite's infrared channels based on sea-surface measurements in the South China Sea. *Journal of Infrared and Millimeter Waves*, **26**, pp. 97–101.

Slater, P.N., Biggar, S.F., Thome, K.J., Gellman, D.I. and Spyak, P.R., 1996, Vicarious radiometric calibrations of EOS sensors. *Journal of Atmospheric and Oceanic Technology*, **13**, pp. 349–359.

Sobrino, J.A., El Kharraze, J. and Li, Z., 2003, Surface temperature and water vapour retrieval from MODIS data. *International Journal of Remote Sensing*, **24**, pp. 5161–5182.

Sobrino, J.A., Jiménez-Muñoz, J.C. and Paolini, L., 2004, Land surface temperature retrieval from LANDSAT TM 5. *Remote Sensing of Environment*, **90**, pp. 434–440.

Tong, J.J., 2004, Study on synthesis radiometric calibration methods for satellite sensors. PhD dissertation, Department of Geography, Beijing Normal University.

Tong, J.J., Qiu, K.M. and Li, X.W., 2004a, Absolute radiometric calibration for thermal infrared channels of FY2B by using NCEP reanalyzed data in Qinghai lake. *IEEE, Geoscience and Remote Sensing Symposium, IGARSS '04. Proceedings*, **6**, pp. 3960–3962, doi:10.1109/IGARSS.2004.1369994.

Tong, J.J., Qiu, K.M. and Li, X.W., 2004b, Absolute radiometric calibration for thermal infrared channels of HY-1/COCTS by using Qinghai Lake. *IEEE, Geoscience and Remote Sensing Symposium, IGARSS '04. Proceedings*, **6**, pp. 3963–3965, doi:10.1109/IGARSS.2004.1369995.

Tong, J.J., Qiu, K.M. and Li, X.W., 2005, New method of in-flight absolute calibration for thermal infrared channels of satellite sensors. *Journal of Infrared and Millimeter Waves*, **24**, pp. 275–280.

Tong, J., Déry, S.J., Hu, B., Chen, Y., Yang, C. and Rong, Z., 2009, On-board real time absolute radiometric calibration for thermal infrared channels of Chinese geostationary meteorological satellites. *Journal of Atmospheric and Oceanic Technology*, **26**, pp. 281–289.

Wang, W.H., Rong, Z.G., Zhang, Y.X. and Hu, X.Q., 2001, Radiometric calibration for the thermal channels of FY-1C and FY-2B. In *The Scientific Research Papers about China Radiometric Calibration Site for Remote Sensing Satellite*, K. Qiu (Ed.), pp. 307–319 (Beijing: Ocean Press).

Xiong, X. and Barnes, W., 2006, An overview of MODIS radiometric calibration and characterization. *Advances in Atmospheric Sciences*, **23**, pp. 69–79.